PRACTICAL IMPLICATIONS OF SONAR TARGET-PHASE MEASUREMENT CLASSIFIERS

PR Atkins — Dept of Electronic Engineering, University of Birmingham, Birmingham B15 2TT
KG Foote — Woods Hole Oceanographic Institution, Woods Hole, Massachusetts 02543, USA
T Collins — Dept of Electronic Engineering, University of Birmingham, Birmingham B15 2TT

1 INTRODUCTION

Active sonar systems normally detect and classify a target based on the amplitude of the received echo strength or the induced Doppler shift. However, additional classification information is available from the phase shift introduced by some targets as a result of the boundary conditions. For example, reverberation returns from the sea surface and from the swimbladders of various fish introduce an additional phase shift that may not be present in returns from an acoustically hard seabed or man-made target. The measurement of target-phase is complicated by the additional phase shifts introduced by the unknown target range and by the phase shifts introduced by Doppler as a result of target and platform motion. Typically, target-phase is estimated by insonifying the target with a signal that contains at least two frequency-scaled components. Thus a more complicated received structure is required that contains a full-band correlator for detection purposes and sub-band correlators for estimating target-phase.

Unfortunately, the unknown phase characteristics of the transducer and electronic circuitry of a sonar system add significantly to the difficulties of target-phase measurements. Calibration procedures based on the use of standard targets normally address only the magnitude response of a system. However, such techniques may be extended to estimate the phase response of a sonar system by the use of suitable transmission signal types. This paper derives two transmission pulse types suitable for measuring target-phase in conjunction with sub-band correlators and presents experimental results for solid standard target spheres.

2 TARGET-PHASE MEASUREMENT AT UNKNOWN RANGES

Consider the case of an incident pressure wave generated by a sonar system and described by $p_{inc} = P_{inc} \exp\left[j(\omega t - k_A r)\right]$ where P_{inc} is the peak incident pressure, ω is the operating frequency, t is time, k_A and k_B are the wavenumbers associated with the media on either side of the encountered boundary, and r is the range from the transmitter, as shown in Figure 1. A reflected wave $p_R = P_R \exp\left[j(\omega t - 2k_A r_0 + k_A r)\right]$ and a transmitted wave $p_T = P_T \exp\left[j(\omega t - k_A r_0 - k_B (r - r_0))\right]$ will be generated where P_R is the peak reflected pressure, P_T is the peak transmitted pressure, r_0 is the range to the boundary wall of the target and collinear geometry is assumed. Assuming planar boundary areas and plane wave insonification, the reflection coefficient can be extracted

$$R = \frac{\rho_B c_B - \rho_A c_A}{\rho_B c_B + \rho_A c_A} \tag{1}$$

where ρ represents the density of the material, c is the sound speed, and ρc is the acoustic impedance of the material. Similarly, the transmission coefficient is given by

$$T = 1 + R = \frac{2\rho_B c_B}{\rho_B c_B + \rho_A c_A}. \tag{2}$$

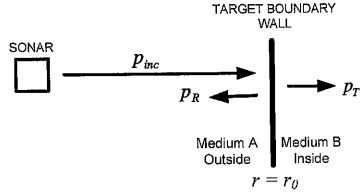

Figure 1. Target at range r_0 insonified by an incident wave

It will be noted that if the acoustic impedance of medium B ($\rho_B c_B$) is less than that of medium A ($\rho_A c_A$), the reflection coefficient will be negative. This implies that for a monostatic sonar system there will be a π-rad phase change occurring for all transmission frequencies whenever the target is acoustically soft. No phase change will be encountered if the target is acoustically hard.

The first reference to measuring target-phase in the field appears to be by Tucker and Barnicle[1], who insonified a target using two harmonically related frequencies and compared the relative phases of the backscattered signals in order to provide additional detection information for the characterisation of fish containing swimbladders. Their technique involved transmitting a low-frequency sinusoidal signal, $p_1 = P_1 \exp(j\omega_1 t)$, and a higher-frequency signal, $p_2 = P_2 \exp(j\omega_2 t)$, where P_1 and P_2 are the peak pressures of the two transmitted components. If the target is located at a range r and introduces a phase shift ϕ, then the pressure at the receive hydrophone (assuming identical outward and return propagation paths) is proportional to

$$p_{RX} = P_1 \exp\left[j\left(\omega_1 t - 2k_1 r + \phi\right)\right] + P_2 \exp\left[j\left(\omega_2 t - 2k_2 r + \phi\right)\right] \tag{3}$$

where k_1 and k_2 are the associated wavenumbers in the water of the low and high frequency signals. The higher-frequency signal will have some fixed relationship to the low-frequency signal, such that $\omega_2 = \mu\omega_1$. Tucker and Barnicle[1] chose a harmonic relationship with $\mu = 2$. The phase comparison of the two received signal components must be made at a common frequency and this was chosen to be that of the higher-frequency signal, ω_2. The receiver structure must isolate the two transmission signals using sub-band processors to generate output signals that are band-limited about centre frequencies ω_1 and ω_2. The phase comparison of the two sub-band transmissions is achieved by frequency-scaling the component corresponding to the time-varying pressure p_1 by the factor μ to obtain a signal

$$p_{Scaling} = \left\{ P_1 \exp\left[j\left(\omega_1 t - 2k_1 r + \phi\right)\right]\right\}^{\mu} = P_1^{\mu} \exp\left[j\mu\left(\omega_1 t - 2k_1 r + \phi\right)\right] \tag{4}$$

The phase comparison is achieved by multiplying the signal $p_{Scaling}$ and the complex-conjugate signal of the higher-frequency transmission component p_2^*.

$$p_{Scaling}\, p_2^* = P_1^{\mu} \exp\left[j\mu\left(\omega_1 t - 2k_1 r + \phi\right)\right] P_2 \exp\left[-j\left(\omega_2 t - 2k_2 r + \phi\right)\right] = P_1^{\mu}\, P_2 \exp\left[j\left(\mu - 1\right)\phi\right] \tag{5}$$

The phase comparison operation generates a signal with a purely real amplitude term $P_1^{\mu}\, P_2$ that will be ignored and a complex term $\exp\left[j\left(\mu-1\right)\phi\right]$ whose argument is proportional to the phase shift introduced by the target. The phase shifts introduced by $\exp\left[j\left(\omega t - 2kr\right)\right]$ due to the time-varying nature of the transmission signal and the unknown target range have been cancelled. The phase term $\exp\left[j\left(\mu-1\right)\phi\right]$, introduced by the target, is related to the separation between the centre frequency of the two sub-bands and any practical implementation should ensure that the value of μ is made as large as possible to reduce the effects of phase noise.

The phase comparison process takes a sinusoid, $\exp\left[j\left(\omega_1 t+n2\pi\right)\right]$ with an unknown phase origin, where n is an integer, and scales it to a higher-frequency, $\exp\left[j\mu\left(\omega_1 t+n2\pi\right)\right]$. The phase of this signal is compared to a higher-frequency signal $\exp\left[j\left(\omega_2 t+l2\pi\right)\right]$, where l is an integer. The resulting phase difference is $(2\pi\mu n) \bmod 2\pi$ which could assume any value. However, the phase difference should be constrained to be part of a finite set of values corresponding to permissible phase sectors. Assuming that M permissible phase sectors are to be used in a system, then $(2\pi\mu nM) \bmod 2\pi = 0$, or $(\mu nM) \bmod 1 = 0$ where M is an integer and $\mu > 1$. The constraint on the ratio of the centre frequency of the two sub-bands, μ , is

$$\mu = \frac{M+N}{M} \text{ where } N \text{ is an integer and } N \geq 1. \qquad (6)$$

In order to conserve bandwidth, an appropriate value of μ, usually chosen from the set $\mu = [2, 3/2, 4/3, 5/3, 5/4, 7/4, 6/5, 7/5]$, would be selected from which it can be deduced that an acoustically hard target echo will fall into one of the $N/(\mu-1)$ hard-phase sectors, whilst a soft target will fall into one of the $N/(\mu-1)$ soft-phase sectors. An additional phase-modulus operation would be used to roll all the received phase samples into a single hard-phase sector, or a single soft-phase sector prior to any decision process.

The block diagram of a typical active sonar system used to measure target-phase is shown in Figure 2. The transmission signal with identifiable information content at frequencies of ω_1 and ω_2 is stored in a look-up table. The received signal is full-band correlated in a conventional manner for target detection purposes. The received signal is also sub-band processed using two correlators, each having the dual-function of optimising the signal-to-noise ratio and ensuring a symmetrical spectral content about the sub-band frequencies in order to obtain components at ω_1 and ω_2. The correlator coefficients are obtained by judicious weighting of the transmission signal. The highest-frequency sub-band (Band 2) is used as the reference channel, whilst the lowest-frequency sub-band (Band 1) is frequency-scaled prior to phase comparison with the reference channel. The use of sub-octave frequency separations introduces ambiguities within the phase measurement process, which, following a careful design approach based on choosing $\mu = [2, 3/2, 4/3, ...]$, will be limited to a finite number of phase sectors. This ambiguity is resolved in conjunction with the output decision process in order to provide a hard-soft decision corresponding to every range cell.

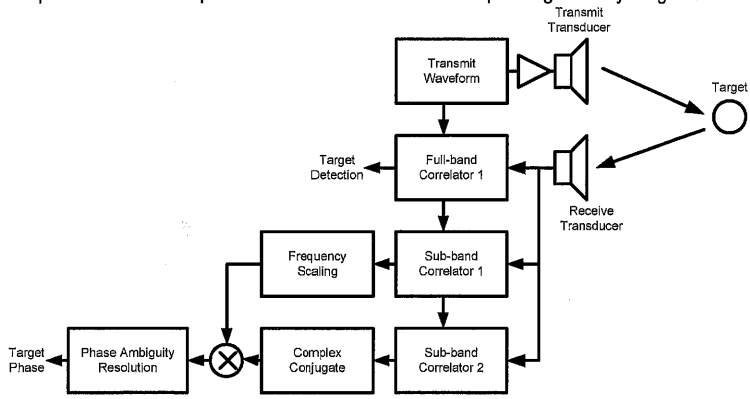

Fig. 2. Block diagram of target-phase estimation sonar

3 EXAMPLES OF POSSIBLE TRANSMISSION SIGNALS

The majority of transmission signals that contain identifiable spectral components at two discrete frequencies may be used for target-phase estimation. Examples included within this section are pulsed continuous wave (CW), sinusoidal frequency-modulated (SFM) and hyperbolic frequency-modulated (HFM). Generally, signals with poor range-resolution capabilities such as CW and SFM would be used for calibration purposes whilst signals such as HFM would be used for operational purposes.

3.1 Pulsed Continuous Wave (CW)

A pulsed CW signal may be described by

$$s(t) = A(t)\exp\left(j\omega_k t\right) \tag{7}$$

where $A(t)$ is the amplitude window function and will initially be assumed to be rectangular $A(t) = rect(t/T)$, k is the sub-band index and the signal is active in the region $-T/2 \le t \le T/2$. The receiver would be based on the FFT algorithm in order to implement a bank of Doppler-matched filters to measure target velocity whilst maintaining detection performance. In a typical operating scenario, a large number of Doppler-shifted propagation paths will be received within a short period of time. Thus the matched filter is always likely to be Doppler-mismatched and the effects of this mismatch should be considered on the performance of the hard-soft estimation technique.

The output of a Doppler-matched filter can be described as

$$\varphi_{xy}(\tau) = \int x(t+\tau)\, y^*(t)\ dt \tag{8}$$

where $x(t+\tau)$ is assumed to be the received signal and $y^*(t)$ is assumed to be the complex conjugate of the replica signal.

Consider the case of one of the sub-band correlators acting on a pulsed, Doppler-shifted CW signal. The analytic signal description of an infinite-extent received signal time-compressed or expanded by an unknown Doppler factor, η, will be $x(t) = \sqrt{\eta}\exp(j\omega\eta t)$ and the complex conjugate infinite-extent replica will be $y^*(t) = \exp(-j\omega t)$. In a practical implementation, the length of the replica used in the receiver will be shorter than the transmitted signal to partially reduce the effects of Doppler overlap losses and to ensure that the receiver determines the spectral content of the processed signals. Thus the limits of the matched filter integration will be $-T/2 \le t \le +T/2$ where T is the receiver replica length

$$\varphi_{xy}(\tau,\eta) = \sqrt{\eta}\int_{-T/2}^{+T/2} \exp\left(j\omega\eta\left(t+\tau\right)\right)\exp\left(-j\omega t\right)\ dt \tag{9}$$

$$\varphi_{xy}(\tau,\eta) = \sqrt{\eta}\, T\exp\left(-j\omega\eta\,\tau\right)\ \mathrm{sinc}\left(\omega T(1-\eta)/2\right). \tag{10}$$

The propagation delay is τ. Equation (10) represents the ambiguity function for an infinite-extent Doppler-mismatched CW signal correlated against a replica of a pulse, using the centre of the replica as the time reference. The envelope remains constant for a change in the range of the target (variations in the value of τ) and varies as a sinc function for changes in the Doppler shift function η. The important parameter to note is the phase shift associated with $\exp(-j\omega\eta\tau)$, which is linearly related to the centre-frequency of the sub-band, ω. Thus calculating the phase of the Doppler-mismatched received signals at two sub-band frequencies and comparing the results will lead to the elimination of the $\exp(-j\omega\eta\tau)$ term.

It can be seen that the phase shifts introduced by Doppler effects and varying ranges within a multi-path cluster are not coupled to the target-induced phase shifts when using a pulsed, dual-frequency, CW signal. The CW signal, or adaptations of it such as the Cox comb[2], represents a good choice of transmission signal for estimating the phase characteristics of the target in a multi-

path, Doppler-spread environment, although the range-resolution is normally unacceptably poor because of the limited bandwidth utilisation.

3.2 Sinusoidal Frequency-Modulated (SFM)

One method of improving range resolution above that of a pulse of CW, whilst maintaining the amplitude of the transmission constant to maximize energy efficiency and compatibility with existing non-linear power amplifiers, is that of transmitting a sinusoidal frequency-modulated (SFM) signal[3]. As SFM signals are adaptations of CW signals, they are suited for measuring target-phase in the presence of target motion. An SFM signal would be generated by the modulation of a carrier signal, ω_0, with a single modulating frequency, ω_m.

$$s(t) = A(t)\exp\left[j\,\omega_0\,t + j\beta\sin\left(j\,\omega_m\,t\right)\right] \qquad 0 \le t \le T \tag{11}$$

where $A(t)$ is the transmit signal window function and β is a modulation constant that defines the bandwidth of the signal. The spectrum of this signal reveals[4] a series of components at frequencies $\omega_0 \pm k\,\omega_m$ where k is an integer in the range $k = 0,1,2..\infty$. Consider the spectrum comprising one set of sidebands shown in Figure 3.

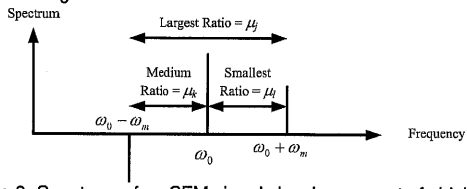

Figure 3. Spectrum of an SFM signal showing one set of sidebands

This signal can provide three ways of measuring the target-phase. The largest frequency separation ratio is between the upper and lower sidebands ($\omega_0 - \omega_m, \omega_0 + \omega_m$), which may be used to measure target-phase with a given frequency-scaling value between the two sub-band correlators, given a value of frequency scaling factor $\mu_j = (M+N)/M$ from equation (6). This defines the modulation frequency as

$$\omega_m = \omega_0 \frac{(\mu_j - 1)}{(\mu_j + 1)} = \omega_0 \frac{(N+M-1)}{(N+M+1)}. \tag{12}$$

The next largest frequency separation ratio is between the carrier and the lower sideband ($\omega_0 - \omega_m, \omega_0$) which provides a frequency-scaling value between the two sub-band corrrelators, μ_k. As a particular example, let μ_k represent a frequency scaling factor

$$\mu_k = \frac{M+N+1}{M+1}. \tag{13}$$

The smallest frequency separation ratio is between the upper sideband and the carrier ($\omega_0, \omega_0 + \omega_m$) which provides a frequency-scaling value between the two sub-band corrrelators, μ_l. As a particular example, let μ_l represent a frequency scaling factor

$$\mu_l = \frac{M+N+2}{M+2}. \tag{14}$$

Each of these three sub-band groupings may be used to provide an estimate of the target-phase and a majority voting decision taken to reduce false classifications[5]. The particular set of relationships defined within equations (12)-(14) can be satisfied when $M \equiv 1$ and thus

$$\omega_m = \omega_0 \frac{N}{(N+2)} \tag{15}$$

An example of using an SFM signal where $N=1$, resulting in $\omega_m = \omega_0/3$, for calibrating the phase response of a transducer will be provided in Section 4.

3.3 Hyperbolic Frequency-Modulated (HFM)

Hyperbolic frequency-modulated signals are often classed as Doppler tolerant because the amplitude of the matched filter response only marginally decreases as a function of target velocity. This Doppler tolerance allows the designer to use a single-correlator receiver implementation. Unfortunately, the Doppler amplitude tolerance of HFM transmissions results in Doppler-induced phase variations that couple to the target-phase and cannot be resolved using a single transmission.

The transmitted signal may be written in the generic form[6]

$$s(t) = A(t)\exp\left(\frac{j}{b}\ln\left(1+b\,\omega_I\,t\right)\right) \qquad 0 \le t \le T \tag{16}$$

where $A(t)$ is the transmit signal window function. The variable $b = (1/\omega_F - 1/\omega_I)/T$ defines a unique sweep factor where ω_I is the start frequency of the transmission sweep, ω_F is the end frequency of the transmission sweep and T is the duration of the transmission sweep.

If the transmitted signal is time-compressed by a factor η, such that the received signal is expressed as $s_R(t) = \sqrt{\eta}\; s(\eta\, t)$, then the output of the receiver may be expressed as[6]

$$s_R(t) = \sqrt{\eta}\; A(\eta\, t)\exp\left(\frac{j2\pi}{b}\ln\left(1+\frac{b}{T}(t-t_D)\right)+j\phi_D\right). \tag{17}$$

The received signal is subject to a constant time delay $t_D = (\eta-1)/(\eta\omega_I\, b)$ and a constant phase shift $\phi_D = \ln(\eta)/b$. The target-phase measurement process uses two sub-bands separated by a frequency ratio of μ. Thus the phase difference between the two sub-band correlator outputs is

$$\theta_{HS} = \frac{(\mu-1)}{b}\ln(\eta) + (\mu-1)\,\phi \tag{18}$$

where ϕ is the phase shift imparted by the target. The phase shift imparted by a Doppler shift and by the target are thus directly coupled. The Doppler-induced phase shift cannot be removed simply as the frequency sweep parameter, b, is fixed for a given single-sweep transmission.

However, the simultaneous transmission of two HFM signals[7] with respective sweep rates of b_1 and b_2 results in a phase difference between the two sub-band correlator outputs of

$$\theta_{HS} = \left(\frac{\mu}{b_1}-\frac{1}{b_2}\right)\ln(\eta) + (\mu-1)\,\phi\,. \tag{28}$$

It will be noted that by ensuring that $b_1 = \mu\, b_2$ the Doppler effects can be cancelled, this results in the desired output of $\theta_{HS} = (\mu-1)\,\phi$.

4 TRANSDUCER CHARACTERISTICS

With the exception of inter-element matching in transducer arrays, the effects of phase are rarely considered within a sonar system. Consider the simplest of electrical-analogue models[8] for a transmit transducer operating near resonance, as illustrated in Figure 4a. The radiation and loss resistance is combined and represented by R_{rad}. The motional impedances are represented by L_{mot} and C_{mot}, whilst the shunt capacitance is represented by C_s. When operated in a transmit mode, a matching circuit would be added to tune-out the shunt capacitance using an inductor, L_1, and a series resistor R_1 to complete the classical electrical filter analogue. When operated in a receive

mode, the resistor R_1 would be removed to improve the overall noise performance and a high-input impedance receive amplifier would be connected to the transducer.

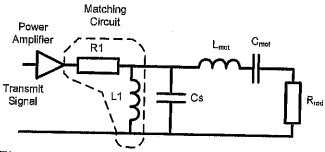

Figure 4a. Transducer in transmit mode

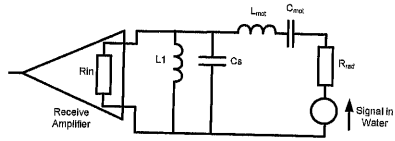

Figure 4b. Transducer in receive mode

The additional phase shifts introduced by this simplistic model are shown in Figure 5a. The correct termination of the transducer during transmission results in a smooth function of phase with respect to frequency. However, during reception the transducer is incorrectly terminated resulting in additional ripples within the phase response. If this transducer were to be used as part of a dual-frequency target-phase measurement system, the measured phase from a point-target would be as illustrated in Figure 5b. The ratio between sub-bands centre frequencies was defined by $\mu = 5/4$ in order to be compatible with a narrow-band transducer with a Q-factor of five. The ideal response would be a straight line coincident with the zero-phase angle axes. The predicted results obtained from the simplest of transducer models will result in an apparent phase distortion that will exceed the classification error bounds of the system.

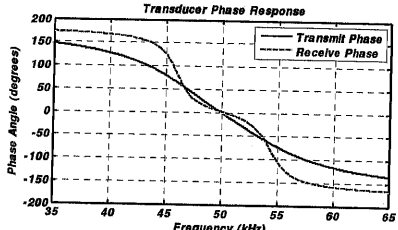

Figure 5a. Additional phase-shifts introduced by the transducer

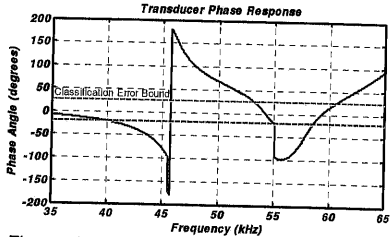

Figure 5b. Relative phase-shift introduced by the transducer when using a dual-frequency transmission signal ($\mu = 5/4$)

Any practical transducer is likely to have a significantly more complicated phase response due to the existence of multiple modes and inter-element coupling. Thus any transducer that is to be used for target-phase classification purposes must be calibrated and compensated prior to use.

5 EXPERIMENTAL RESULTS

There are many ways of calibrating a transducer[9], but for this application the techniques traditionally used for calibrating scientific echo sounders[10] were adopted. A 75-mm-diameter sphere made of tungsten carbide with a 6% cobalt binder was selected as the standard target. An analytical model for the scattering of a plane acoustic wave based on that of Goodman and Stern[11] was used to predict the acoustic characteristics of the standard target. The transducer requiring calibration and phase-compensation was a Reson TC2116 operating over a frequency range 25 – 150 kHz. The experimental setup is shown in Figure 6 with the standard target being suspended approximately 2 m below the TC2116 transducer. A sense-hydrophone consisting of a ball-hydrophone of nominal diameter 12.7 mm was suspended approximately 1 m below the projector in order to measure the incident and backscattered fields.

The range-corrected phase response of the standard target measured using the sense-hydrophone is shown as a black trace in Figure 7. The predicted phase-response was computed for a water temperature of 18°C, mass density of 998 g kg/m^3 and sound speed of 1476 m/s and assuming

continuous excitation. The continuously excited case was then convolved with the transmission signal characteristics (a whole number of cycles within a pulse) to obtain the predicted calibration response shown as a red trace. The agreement between experimental and predicted phase-responses of the target sphere appears to be satisfactory. The use of a sense-hydrophone effectively results in a self-correcting methodology as the unknown phase response of the ball-hydrophone is cancelled when taking the difference between insonified and reflected fields.

When using the main Reson TC2116 transducer, the phase-distortion effects of the electronics as well as the transducer will combine to produce the received phase result shown as the black trace in Figure 8. The characteristics of the standard target may be subtracted to yield the underlying effects of the transducer and electronics as indicated by the red trace. The equivalent threshold limits for a dual-frequency phase measurement system based on $\mu = 5/4$ are also depicted, clearly showing that classification errors would arise from the use of an uncompensated transducer.

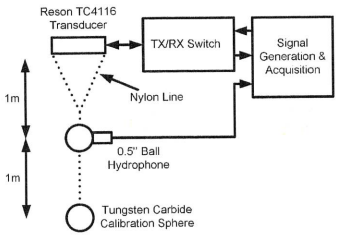

Figure 6. Experimental setup

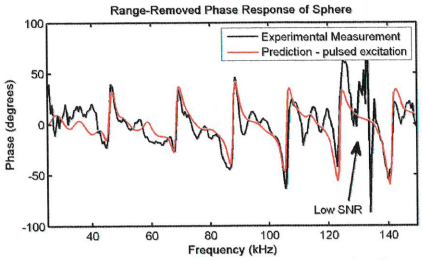

Figure 7. Measured phase response of sphere

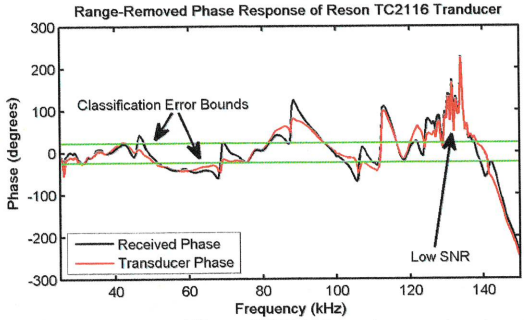

Figure 8. Phase response of Reson TC2116 transducer and system electronics

6 CONCLUSIONS

The concept of using a dual-frequency transmission signal to measure the phase response of a target has been introduced. Transmission signal types such as hyperbolic frequency-modulated chirps may be adapted for measuring target-phase whilst maintaining good range resolution. However, it is essential that the phase characteristics of the sonar system are measured and compensated before such techniques have any practical use. The application of sinusoidal frequency-modulated signals in conjunction with standard targets for the *in situ* calibration of a sonar system has been demonstrated.

7 REFERENCES

1. D.G. Tucker and N.J. Barnicle, "Distinguishing automatically the echoes from acoustically 'hard' and 'soft' objects with particular reference to the detection of fish," *J. Sound Vib.* 9, pp. 393-397, May 1969.
2. H. Cox and H. Lai, "Geometric comb waveforms for reverberation suppression," *Proceedings of the Twenty -Eighth Asimolar Conference on Signal, Systems and Computers*, Vol. 2, pp. 1154-1189, October 1994.
3. T. Collins and P.R. Atkins, "Doppler-sensitive active sonar pulse designs for reverberation processing," *IEE Proc. Radar, Sonar Navig.*, Vol. 145, pp. 347-353, December 1998.
4. A. B. Carlson, P. B. Crilly, and J. C. Rutledge, "Communication Systems, An Introduction to Signals and Noise in Electrical Communication," New York, McGraw Hill, 2001.
5. S.D. Milligan, L.R. LeBlanc and F.H. Middleton, "Statistical grouping of acoustic reflection profiles," *J. Acoust. Soc. Am.* 64, pp. 795-807, Sept. 1978.
6. J.J. Kroszczynski, "Pulse Compression by Means of Linear Period Modulation," *Proc. IEEE*, Vol.57, No. 7, pp. 1260-1266, July 1969.
7. P.R. Atkins, T. Collins, and K.G. Foote, "Transmit-signal Design and Processing Strategies for Sonar Target Phase Measurement," *Proc. IEEE Selected Topics in Signal Processing*, Vol.1, No. 1, pp. 91-104, June 2007.
8. D. Stansfield, "Underwater Electroacoustic Transducers," Bath University Press, 1991.
9. R.J. Bobber, "Underwater electroacoustic measurements" (Naval Research Laboratory, Washington, DC, 1970).
10. K.G. Foote, H.P. Knudsen, G. Vestnes, D.N. MacLennan, and E.J. Simmonds, "Calibration of acoustic instruments for fish density estimation: a practical guide," ICES Coop. Res. Rep., (144), 69 pp (1987).
11. R.R. Goodman and R. Stern, "Reflection and transmission of sound by elastic spherical shells," J. Acoust. Soc. Am., 34, 338-344 (1962).